Mechanical Engineering Research; Vol. 5, No. 2; 2015
ISSN 1927-0607 E-ISSN 1927-0615
Published by Canadian Center of Science and Education

Incremental Inverse Kinematics of Wire-Suspended Parallel Mechanical System Taking into Account Many-Worlds Situation

Kazuyuki Hanahara[1]

[1] Graduate School of System Informatics, Kobe University, Kobe, Japan

Correspondence: Kazuyuki Hanahara, Graduate School of System Informatics, Kobe University, Kobe, Japan. Tel: 81-78-803-6249. E-mail: hanahara@cs.kobe-u.ac.jp

Received: July 13, 2015 Accepted: August 4, 2015 Online Published: August 7, 2015

doi:10.5539/mer.v5n2p24 URL: http://dx.doi.org/10.5539/mer.v5n2p24

Abstract

Wire-suspended platform is a parallel mechanical system consisting of a rigid platform and a number of length-adjustable wires. In order to deal with the kinematics of this type of mechanical system, we have to take into account the conspicuous characteristic of a wire that it can take only a tensile force. It has been demonstrated in the previous studies that this leads to plural possible kinematic states corresponding to a given set of wire lengths. In this study, we formulate an inverse kinematics problem in an incremental form based on the linearization of the kinematic relation of the system. Displacement of the mass center position of the platform is also taken into account for the articulation variables, in addition to the wire member lengths. A solution procedure that deals with the many-worlds situation is developed under the assumption of some adequate sensing devices. Numerical experiments based on computer simulation are carried out and the feasibility of the proposed approach is demonstrated with the attained kinematic motions of the simulated platform system.

Keywords: parallel mechanism, wire, inverse kinematics, many-worlds interpretation, Interval arithmetic

1. Introduction

Parallel robots (Merlet, 2006) or platforms (Stewart, 1965-66) have a number of different features compared with the conventional serial robotic mechanisms. One of such features is that they can have a number of non-rigid links of wire or cable. A platform supported by a number of wires or cables, which are actuated and length-adjustable, is a typical mechanical system of this type. Such mechanical systems are referred to as robocrane (Albus et al., 1992), wire-actuated parallel manipulator (Agahi & Notash, 2009), wire-driven parallel mechanism (Yamaguchi et al., 2004), cable robot (Ghasemi et al., 2009) (Borgstrom et al., 2009), cable-driven robot (Bosscher et al., 2006), cable-driven parallel robot (Tadokoro et al., 2003) (Carricato & Merlet 2013) (Carricato, 2013), cable-suspended robot (Roberts et al., 1998) (Oh & Agrawal, 2005), cable-suspended parallel robot (Pusey et al., 2004), cable-driven parallel mechanism (Perreault & Gosselin, 2008), tendon-based manipulator (Hiller et al., 2005), and so on. In this study, we refer this type of mechanical system to as a wire-suspended platform (Hanahara, 2015). A mechanical system of this type is well represented by a suspended platform of rigid body, a number of length-adjustable wires for the suspension, and the corresponding fixed connection points of the wires at the wall or at the ceiling. In order to control the six degrees of freedom (DOFs) in 3D space, or the three DOFs in 2D space, of the position and orientation of the platform, it is natural that the number of wires is six or three. However, such a mechanical system having less wires is possible (Carricato & Merlet, 2013) (Carricato, 2013); the equilibrium condition determines the position and orientation to be attained by the platform in this case. In contrast to the platform system consisting only of rigid links, a platform having a redundant number of wires (Oh & Agrawal, 2005) is also possible without difficulty.

There are several issues that have to be taken into consideration in the case of dealing with the kinematics of mechanical system of this type: the conspicuous characteristic of a wire that they cannot support any compressive force, the static equilibrium condition under gravity and the influence of displacement of mass center of the platform. The previous study (Hanahara, 2015) deals with these issues and shows a general formulation and the solution of the incremental forward kinematics problem of wire-suspended platform based on the interval arithmetic (Moore et al., 2009) as well as the many-worlds interpretation (Vaidman, 2008). It has been demonstrated that even in this linearized incremental case, the possible configuration of the platform is not unique in general; we have to deal with the plural possibilities simultaneously.

We deal with the inverse kinematics of mechanical system of this type. We adopt the approach developed in the previous study, which is based on the incremental formulation with the interval arithmetic and the many-worlds interpretation. We assume that some sort of sensing device is available in the current study, since the formulated incremental inverse kinematics problem has often no feasible solutions without confining the kinematical possibilities, which are to be obtained as the consequence of the many-worlds interpretation. It should be noted that the unavoidable error in the measurement results of the sensors is naturally taken into account in the form of the interval in our approach.

We conduct a number of numerical experiments with a simulated platform system assumed to have simple binary tension sensors. The feasibility of the proposed incremental inverse kinematics approach as well as the obtained characteristic behavior of the wire-suspended platform is demonstrated.

2. Incremental Forward Kinematics Based on Many-Worlds Interpretation

In order to make the article self-contained, we summarize the incremental forward kinematics problem of the wire-suspended platform as well as the management of the solution based on the many-worlds interpretation.

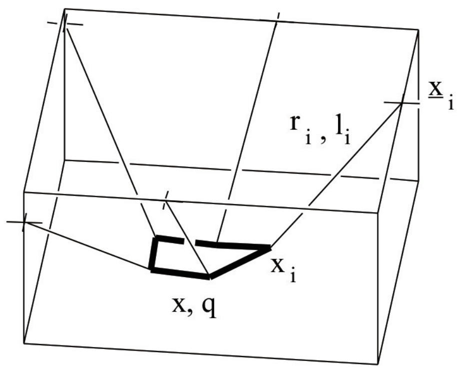

Figure 1. Conceptual illustration of wire-actuated platform

2.1 Basic Equation in General Form

Figure 1 shows the conceptual illustration of the wire-suspended platform system dealt with in the current study; a platform of rigid body is suspended by a number of length-adjustable wires from the fixed connection points. We deal with the kinematics of the system based on the following two basic equations in general form:

$$\boldsymbol{l} = \boldsymbol{l}(\boldsymbol{X}) \tag{1}$$

$$\boldsymbol{F} = \boldsymbol{F}(\boldsymbol{X}, \boldsymbol{\tau}, \hat{\boldsymbol{c}}) = 0 \tag{2}$$

Equation (1) is the geometry condition and Eq.(2) is the equilibrium condition under the gravity. In these equations, $\boldsymbol{l} = [l_1, \cdots, l_N]^T$ and l_i is the distance between the fixed connection point $\underline{\boldsymbol{x}}_i$ and the connection point $\boldsymbol{x}_i$ at the platform, which is referred to as the geometrical length of i-th wire, $\boldsymbol{X} = [\boldsymbol{x}^T, \boldsymbol{\theta}^T]^T$ denotes the position and orientation of the platform, $\boldsymbol{F} = [\boldsymbol{f}^T, \boldsymbol{\eta}^T]^T$ denotes the force and moment acting on the platform, $\boldsymbol{\tau} = [\tau_1, \cdots, \tau_N]^T$ and τ_i is the tension of the i-th wire and $\hat{\boldsymbol{c}}$ is the position of the mass center of the platform referring to the platform-fixed coordinate. Note that $\hat{\boldsymbol{c}}$ is not assumed constant in this study.

The following two conditions have to be satisfied for a wire-suspended system:

$$\boldsymbol{\rho} \geq \boldsymbol{l} \tag{3}$$

$$\boldsymbol{\tau} \geq 0 \tag{4}$$

where $\boldsymbol{\rho} = [\rho_1, \cdots, \rho_N]^T$ and ρ_i is the kinematical length of the i-th wire, that is, the wire length directly controlled by the actuation mechanism. Equation (3) is the geometrical constraint for the wire lengths and Eq.(4) denotes that the tension in a wire must have a positive value.

The following incremental relations of Eqs.(1) and (2) are used in this study:

$$\Delta \boldsymbol{l} = \frac{\partial \boldsymbol{l}}{\partial \boldsymbol{X}} \Delta \boldsymbol{X} \tag{5}$$

$$\Delta \boldsymbol{F} = \frac{\partial \boldsymbol{F}}{\partial \boldsymbol{X}} \Delta \boldsymbol{X} + \frac{\partial \boldsymbol{F}}{\partial \boldsymbol{\tau}} \Delta \boldsymbol{\tau} + \frac{\partial \boldsymbol{F}}{\partial \hat{\boldsymbol{c}}} \Delta \hat{\boldsymbol{c}} \tag{6}$$

The detail of the formulation of Eqs.(1) and (2) as well as their incremental relations (5) and (6) for the general case of the wire-suspended platform system is given in (Hanahara, 2015).

2.2 Incremental Forward Kinematics Solution

The forward kinematics based on the increment $\Delta \boldsymbol{\rho}$ in wire lengths and the displacement $\Delta \hat{\boldsymbol{c}}$ in platform mass center position is calculated based the following equilibrium condition in incremental form taking into account the unbalanced force $\boldsymbol{F}_\epsilon$ to be balanced:

$$\boldsymbol{F}_\epsilon + \frac{\partial \boldsymbol{F}}{\partial \boldsymbol{X}} \Delta \boldsymbol{X} + \frac{\partial \boldsymbol{F}}{\partial \boldsymbol{\tau}} \Delta \boldsymbol{\tau} + \frac{\partial \boldsymbol{F}}{\partial \hat{\boldsymbol{c}}} \Delta \hat{\boldsymbol{c}} = 0 \tag{7}$$

The geometrical and tension constraints (3) and (4) in the incremental form are expressed as

$$\boldsymbol{\rho} + \Delta \boldsymbol{\rho} \geq \boldsymbol{l} + \frac{\partial \boldsymbol{l}}{\partial \boldsymbol{X}} \Delta \boldsymbol{X} \tag{8}$$

$$\boldsymbol{\tau} + \Delta \boldsymbol{\tau} \geq 0 \tag{9}$$

The incremental forward kinematics problem is to find $\Delta \boldsymbol{X}$ and $\Delta \boldsymbol{\tau}$ corresponding to given $\Delta \boldsymbol{\rho}$ and $\Delta \hat{\boldsymbol{c}}$ that satisfy Eqs.(7), (8) and (9).

The tension state of the wires is denoted by the two sets: A for taut wires and S for slack wires. Assuming the tension state of wires A and S after the kinematic increment, the equilibrium condition (7) is rewritten as

$$\frac{\partial \boldsymbol{F}}{\partial \boldsymbol{X}} \Delta \boldsymbol{X} + \frac{\partial \boldsymbol{F}}{\partial \boldsymbol{\tau}_\mathsf{A}} \Delta \boldsymbol{\tau}_\mathsf{A} = \Delta \boldsymbol{F}_{\tau_\mathsf{S} \hat{c}} \tag{10}$$

where

$$\Delta \boldsymbol{F}_{\tau_\mathsf{S} \hat{c}} = -\boldsymbol{F}_\epsilon - \frac{\partial \boldsymbol{F}}{\partial \boldsymbol{\tau}_\mathsf{S}} \Delta \boldsymbol{\tau}_\mathsf{S} - \frac{\partial \boldsymbol{F}}{\partial \hat{\boldsymbol{c}}} \Delta \hat{\boldsymbol{c}} \tag{11}$$

The tension increment vector for wires to be slack is immediately determined as

$$\Delta \boldsymbol{\tau}_\mathsf{S} = -\boldsymbol{\tau}_\mathsf{S} \quad (\because \boldsymbol{\tau}_\mathsf{S} + \Delta \boldsymbol{\tau}_\mathsf{S} = 0) \tag{12}$$

For the wires to be taut, the following equation is then obtained as a part of the geometrical condition (8):

$$\frac{\partial \boldsymbol{l}_\mathsf{A}}{\partial \boldsymbol{X}} \Delta \boldsymbol{X} = \Delta \boldsymbol{l}_\mathsf{A} \tag{13}$$

where

$$\Delta \boldsymbol{l}_\mathsf{A} = \boldsymbol{\rho}_\mathsf{A} + \Delta \boldsymbol{\rho}_\mathsf{A} - \boldsymbol{l}_\mathsf{A} \tag{14}$$

On the basis of Eqs.(10) and (13), the following equation is obtained:

$$\boldsymbol{J} \Delta \boldsymbol{v} = \Delta \boldsymbol{z} \tag{15}$$

where

$$\boldsymbol{J} = \begin{bmatrix} \dfrac{\partial \boldsymbol{F}}{\partial \boldsymbol{X}} & \dfrac{\partial \boldsymbol{F}}{\partial \boldsymbol{\tau}_\mathsf{A}} \\ \dfrac{\partial \boldsymbol{l}_\mathsf{A}}{\partial \boldsymbol{X}} & 0 \end{bmatrix} \tag{16}$$

is the combined Jacobian matrix and

$$\Delta \boldsymbol{v} = \begin{bmatrix} \Delta \boldsymbol{X} \\ \Delta \boldsymbol{\tau}_\mathsf{A} \end{bmatrix}, \quad \Delta \boldsymbol{z} = \begin{bmatrix} \Delta \boldsymbol{F}_{\tau_\mathsf{S} \hat{c}} \\ \Delta \boldsymbol{l}_\mathsf{A} \end{bmatrix} \tag{17}$$

are the corresponding known and unknown vectors. Equation (15) can be solved as

$$\Delta \boldsymbol{v} = \boldsymbol{J}^{-1} \Delta z \tag{18}$$

We denote the interior of the matrix $\boldsymbol{J}^{-1}$ in Eq.(18) as

$$\boldsymbol{J}^{-1} = \begin{bmatrix} \dfrac{\partial \boldsymbol{X}}{\partial \boldsymbol{F}} & \dfrac{\partial \boldsymbol{X}}{\partial \boldsymbol{l}_{\mathsf{A}}} \\ \dfrac{\partial \boldsymbol{\tau}_{\mathsf{A}}}{\partial \boldsymbol{F}} & \dfrac{\partial \boldsymbol{\tau}_{\mathsf{A}}}{\partial \boldsymbol{l}_{\mathsf{A}}} \end{bmatrix} \tag{19}$$

It should be noted that $\dfrac{\partial \boldsymbol{X}}{\partial \boldsymbol{F}} \neq \left(\dfrac{\partial \boldsymbol{F}}{\partial \boldsymbol{X}}\right)^{-1}$, $\dfrac{\partial \boldsymbol{X}}{\partial \boldsymbol{l}_{\mathsf{A}}} \neq \left(\dfrac{\partial \boldsymbol{l}_{\mathsf{A}}}{\partial \boldsymbol{X}}\right)^{-1}$ and $\dfrac{\partial \boldsymbol{\tau}_{\mathsf{A}}}{\partial \boldsymbol{F}} \neq \left(\dfrac{\partial \boldsymbol{F}}{\partial \boldsymbol{\tau}_{\mathsf{A}}}\right)^{-1}$ in general even in the case that $\mathrm{Dim}(\boldsymbol{l}_{\mathsf{A}}) = \mathrm{Dim}(\boldsymbol{X})$ since these are obtained as the partial matrices of $\boldsymbol{J}^{-1}$. These notations are consistently used as the same meanings in this paper. On the basis of the expression in Eq.(19), Eq.(18) is rewritten as

$$\Delta \boldsymbol{X} = \frac{\partial \boldsymbol{X}}{\partial \boldsymbol{F}} \Delta \boldsymbol{F}_{\tau_{\mathsf{S}}\hat{c}} + \frac{\partial \boldsymbol{X}}{\partial \boldsymbol{l}_{\mathsf{A}}} \Delta \boldsymbol{l}_{\mathsf{A}} \tag{20}$$

$$\Delta \boldsymbol{\tau}_{\mathsf{A}} = \frac{\partial \boldsymbol{\tau}_{\mathsf{A}}}{\partial \boldsymbol{F}} \Delta \boldsymbol{F}_{\tau_{\mathsf{S}}\hat{c}} + \frac{\partial \boldsymbol{\tau}_{\mathsf{A}}}{\partial \boldsymbol{l}_{\mathsf{A}}} \Delta \boldsymbol{l}_{\mathsf{A}} \tag{21}$$

The increment $\Delta \boldsymbol{X}$ has to satisfy the following geometrical condition for the slack wires, which is a part of Eq.(8):

$$\boldsymbol{\rho}_{\mathsf{S}} + \Delta \boldsymbol{\rho}_{\mathsf{S}} \geq \boldsymbol{l}_{\mathsf{S}} + \frac{\partial \boldsymbol{l}_{\mathsf{S}}}{\partial \boldsymbol{X}} \Delta \boldsymbol{X} \tag{22}$$

The increment $\Delta \boldsymbol{\tau}_{\mathsf{A}}$ has to satisfy the following condition for the taut wires, which is a part of Eq.(9):

$$\boldsymbol{\tau}_{\mathsf{A}} + \Delta \boldsymbol{\tau}_{\mathsf{A}} \geq 0 \tag{23}$$

In the case that the both conditions (22) and (23) are satisfied, the incremental forward kinematics problem based on the given increments $\Delta \boldsymbol{\rho}$ and $\Delta \hat{\boldsymbol{c}}$ is solved under the tension state assumption of A and S and the solution increments $\Delta \boldsymbol{X}$ and $\Delta \boldsymbol{\tau}$ are obtained, where the tension increment vector $\Delta \boldsymbol{\tau}$ is obtained partially as $\Delta \boldsymbol{\tau}_{\mathsf{A}}$ and partially as $\Delta \boldsymbol{\tau}_{\mathsf{S}}$. It is also possible to deal with the case that $\boldsymbol{J}$ is singular in a similar manner (Hanahara, 2015).

2.3 Interval Arithmetic Approach

It is practically impossible to eliminate measurement error in the wire lengths as well as in the platform mass center position. In the current study, we deal with these values in the form of interval (Moore et al., 2009) as

$$[\boldsymbol{\rho}] = \boldsymbol{\rho} + [\boldsymbol{\rho}_{\mathrm{err}}], \quad [\hat{\boldsymbol{c}}] = \hat{\boldsymbol{c}} + [\hat{\boldsymbol{c}}_{\mathrm{err}}] \tag{24}$$

where $[\boldsymbol{\rho}_{\mathrm{err}}]$ and $[\hat{\boldsymbol{c}}_{\mathrm{err}}]$ denote the uncertainty magnitude of $\boldsymbol{\rho}$ and $\hat{\boldsymbol{c}}$; the actual error values are bounded as follows:

$$\underline{[\boldsymbol{\rho}_{\mathrm{err}}]} \leq \boldsymbol{\rho}_{\mathrm{err}} \leq \overline{[\boldsymbol{\rho}_{\mathrm{err}}]}, \quad \underline{[\hat{\boldsymbol{c}}_{\mathrm{err}}]} \leq \hat{\boldsymbol{c}}_{\mathrm{err}} \leq \overline{[\hat{\boldsymbol{c}}_{\mathrm{err}}]}$$

Calculating equations in the previous section by taking into account these interval values, Eqs.(20) and (21) are rewritten in the following form as

$$[\Delta \boldsymbol{X}] = \frac{\partial \boldsymbol{X}}{\partial \boldsymbol{F}} [\Delta \boldsymbol{F}_{\tau_{\mathsf{S}}\hat{c}}] + \frac{\partial \boldsymbol{X}}{\partial \boldsymbol{l}_{\mathsf{A}}} [\Delta \boldsymbol{l}_{\mathsf{A}}] \tag{25}$$

$$[\Delta \boldsymbol{\tau}_{\mathsf{A}}] = \frac{\partial \boldsymbol{\tau}_{\mathsf{A}}}{\partial \boldsymbol{F}} [\Delta \boldsymbol{F}_{\tau_{\mathsf{S}}\hat{c}}] + \frac{\partial \boldsymbol{\tau}_{\mathsf{A}}}{\partial \boldsymbol{l}_{\mathsf{A}}} [\Delta \boldsymbol{l}_{\mathsf{A}}] \tag{26}$$

The interval of the geometrical wire lengths increment corresponding to the slack wires is obtained as

$$[\Delta \boldsymbol{l}_{\mathsf{S}}] = \frac{\partial \boldsymbol{l}_{\mathsf{S}}}{\partial \boldsymbol{X}} [\Delta \boldsymbol{X}] \tag{27}$$

Referring to the non-interval geometrical condition (22) for the slack wires, the following condition is obtained:

$$\overline{[\rho_{\mathsf{S}}]} + \Delta\rho_{\mathsf{S}} \geq \boldsymbol{l}_{\mathsf{S}} + \underline{[\Delta \boldsymbol{l}_{\mathsf{S}}]} \tag{28}$$

Similarly, the following condition for the taut wires is obtained based on the non-interval condition (23):

$$\boldsymbol{\tau}_{\mathsf{A}} + \overline{[\Delta\boldsymbol{\tau}_{\mathsf{A}}]} \geq 0 \tag{29}$$

In the case that the both conditions (28) and (29) are satisfied, the incremental forward kinematics has the possibility to be feasible under the tension state assumption of A and S.

2.4 Many-Worlds Interpretation

This interval-based incremental forward kinematics leads to a number of possible solutions each of which corresponds to different tension states. In order to cope with the situation, a kind of parallelism referred to as many-worlds interpretation is adopted to deal with the possible states simultaneously. The phrase 'many-worlds interpretation' is taken from the quantum mechanics theory (e.g. Vaidman, 2008); in brief, the interpretation says that each of the different possible states belongs to its corresponding different world and all of these worlds exist simultaneously.

In the incremental kinematics based on the many-worlds interpretation, basically, we deal with all the possible states as evenly actual and existent. It should be noted, however, that we also adopt the so-called unification process in order to suppress the number of possible states from the practicality point of view. The detail is also discussed in (Hanahara, 2015).

3. Formulation of Inverse Kinematics Problem

Taking into account the situation of the many-worlds interpretation, the inverse kinematics of the wire-suspended platform has to deal with the plural possible kinematic states.

3.1 How to Deal with the Problem

The inverse kinematics of the wire-suspended platform in incremental form is to find the increment $\Delta\boldsymbol{\rho}$ in kinematic wire lengths as well as the increment $\Delta\hat{\boldsymbol{c}}$ in platform mass center position, that is corresponding to the desired incremental motion of the platform. An important issue that has to be taken into consideration in this study is that the desired increment $\underline{\Delta\boldsymbol{X}}$ in platform position and orientation itself differs in accordance with the kinematic state of respective possibilities. It should be noted that the increments $\Delta\boldsymbol{\rho}$ and $\Delta\hat{\boldsymbol{c}}$ are common to all the possibilities under consideration but the desired increment $\underline{\Delta\boldsymbol{X}}$ is specific to each possibility; that is, it is generally impossible to find $\Delta\boldsymbol{\rho}$ and $\Delta\hat{\boldsymbol{c}}$ that meet various values of $\underline{\Delta\boldsymbol{X}}$ of all the possibilities. On the basis of the consideration, we deal with the inverse kinematics problem as a minimization problem. The difference between the desired platform position and orientation and the platform positions and orientations attained by the respective possibilities under consideration is adopted as the objective function to be minimized.

3.2 Formulation as Minimization Problem

Suppose we have P possibilities of kinematic states, which are obtained as the result of forward kinematics calculation. Sensor information such as the wire tension values as well as the platform position and orientation should be adopted. Accordingly, we confine the number of possible kinematic states to be taken into account for the inverse kinematics to $P' \leq P$ by means of the sensor information.

For the p-th possible kinematic state ($p = 1, \cdots, P'$) taken into account for the inverse kinematics in the current incremental step, the equilibrium condition (7) is expressed as follows:

$$\boldsymbol{F}_{\epsilon}^{(p)} + \frac{\partial \boldsymbol{F}}{\partial \boldsymbol{X}}^{(p)} \Delta\boldsymbol{X}^{(p)} + \frac{\partial \boldsymbol{F}}{\partial \boldsymbol{\tau}}^{(p)} \Delta\boldsymbol{\tau}^{(p)} + \frac{\partial \boldsymbol{F}}{\partial \hat{\boldsymbol{c}}}^{(p)} \Delta\hat{\boldsymbol{c}} = 0 \tag{30}$$

where superscript (p) denotes that the values are specific to the p-th possibility. It should be noted that the increment $\Delta\hat{\boldsymbol{c}}$ in platform mass center position referring to the platform-fixed coordinate is common to all the possibilities. Similarly, the geometrical condition (8) is rewritten as

$$\boldsymbol{\rho} + \Delta\boldsymbol{\rho} \geq \boldsymbol{l}^{(p)} + \frac{\partial \boldsymbol{l}}{\partial \boldsymbol{X}}^{(p)} \Delta\boldsymbol{X}^{(p)} \tag{31}$$

Note that the kinematical wire lengths $\boldsymbol{\rho}$ and its increment $\Delta\boldsymbol{\rho}$ are common to all the possibilities as well.

Assuming the tension state $\mathsf{A}^{(p)}$ and $\mathsf{S}^{(p)}$ for the p-th possible kinematic state after the increment, the equilibrium condition (30) is rewritten as

$$\frac{\partial \boldsymbol{F}}{\partial \hat{\boldsymbol{c}}}^{(p)} \Delta\hat{\boldsymbol{c}} + \frac{\partial \boldsymbol{F}}{\partial \boldsymbol{X}}^{(p)} \Delta\boldsymbol{X}^{(p)} + \frac{\partial \boldsymbol{F}}{\partial \boldsymbol{\tau}_{\mathsf{A}}}^{(p)} \Delta\boldsymbol{\tau}_{\mathsf{A}}^{(p)} = -\boldsymbol{F}_{\epsilon}^{(p)} - \frac{\partial \boldsymbol{F}}{\partial \boldsymbol{\tau}_{\mathsf{S}}}^{(p)} \Delta\boldsymbol{\tau}_{\mathsf{S}}^{(p)} \tag{32}$$

In order to be exact, the subscripts A and S in Eq.(32) should be denoted as $\mathsf{A}^{(p)}$ and $\mathsf{S}^{(p)}$; however, the superscript (p) for these subscripts are omitted for the sake of simplicity. Similarly, the geometrical condition (31) is rewritten separately for the taut and slack wires as

$$-\Delta\boldsymbol{\rho}_{\mathsf{A}^{(p)}} + \frac{\partial \boldsymbol{l}_{\mathsf{A}}}{\partial \boldsymbol{X}}^{(p)} \Delta\boldsymbol{X}^{(p)} \;=\; \boldsymbol{\rho}_{\mathsf{A}^{(p)}} - \boldsymbol{l}_{\mathsf{A}}^{(p)} \tag{33}$$

$$\frac{\partial \boldsymbol{l}_{\mathsf{S}}}{\partial \boldsymbol{X}}^{(p)} \Delta\boldsymbol{X}^{(p)} + \boldsymbol{l}_{\mathsf{S}}^{(p)} \;\leq\; \Delta\boldsymbol{\rho}_{\mathsf{S}^{(p)}} + \boldsymbol{\rho}_{\mathsf{S}^{(p)}} \tag{34}$$

It should be noted that the superscript (p) of the subscripts A and S for $\boldsymbol{\rho}$ and $\Delta\boldsymbol{\rho}$ should not be omitted in the above equations, since the *values* are common to all the possibilities but the *tension state* is specific to each of the possibilities. The tension constraint in incremental form (9) is similarly rewritten as

$$\boldsymbol{\tau}^{(p)} + \Delta\boldsymbol{\tau}^{(p)} \geq 0 \tag{35}$$

Taking into account all of the possible kinematic states under consideration, we introduce the following objective function to be minimized for platform position and orientation:

$$g_X = \frac{1}{P'} \sum_{p=1}^{P'} \frac{1}{2} \left(\Delta\boldsymbol{X}^{(p)} - \underline{\Delta\boldsymbol{X}^{(p)}}\right)^T \begin{bmatrix} K_x\boldsymbol{I} & 0 \\ 0 & K_\theta\boldsymbol{I} \end{bmatrix} \left(\Delta\boldsymbol{X}^{(p)} - \underline{\Delta\boldsymbol{X}^{(p)}}\right) \tag{36}$$

where

$$\underline{\Delta\boldsymbol{X}^{(p)}} = \underline{\boldsymbol{X}} - \boldsymbol{X}^{(p)} \tag{37}$$

is the target value expressed in terms of the specified platform position and orientation $\underline{\boldsymbol{X}}$ at the current incremental step, K_x and K_θ are the penalty coefficients respectively corresponding to position and orientation, and $\boldsymbol{I}$ is the three-dimensional identity matrix. The following auxiliary objective functions are also introduced:

$$g_{\rho\hat{c}} \;=\; \frac{1}{2}K_\rho \Delta\boldsymbol{\rho}^T \Delta\boldsymbol{\rho} + \frac{1}{2}K_{\hat{c}} \Delta\hat{\boldsymbol{c}}^T \Delta\hat{\boldsymbol{c}} \tag{38}$$

$$g_\tau \;=\; \frac{1}{P} \sum_{p=1}^{P} \frac{1}{2} K_\tau (\Delta\boldsymbol{\tau}_{\mathsf{A}}^{(p)} - \underline{\Delta\boldsymbol{\tau}_{\mathsf{A}}^{(p)}})^T (\Delta\boldsymbol{\tau}_{\mathsf{A}}^{(p)} - \underline{\Delta\boldsymbol{\tau}_{\mathsf{A}}^{(p)}}) \tag{39}$$

with the weight coefficients K_ρ, $K_{\hat{c}}$ and K_τ. Equation (38) is introduced intended to suppress the eccentricity of the increments in wire lengths as well as the platform mass center position. Equation (39) is introduced to avoid extreme values of wire tensions, where

$$\underline{\Delta\boldsymbol{\tau}_{\mathsf{A}}^{(p)}} = \underline{\boldsymbol{\tau}}_{\mathsf{A}^{(p)}} - \boldsymbol{\tau}_{\mathsf{A}}^{(p)} \tag{40}$$

and $\underline{\boldsymbol{\tau}}$ is an adequate reference tension value vector.

On the basis of these objective functions, the incremental inverse kinematics problem is formulated as

$$\begin{array}{lll} \text{Minimize} \quad g = g_X + g_{\rho\hat{c}} + g_\tau & \text{with respect to} & \Delta\boldsymbol{\rho}, \Delta\hat{\boldsymbol{c}}, \Delta\boldsymbol{X}^{(p)}, \Delta\boldsymbol{\tau}_{\mathsf{A}}^{(p)}\ (p = 1, \cdots, P') \\ & \text{subject to} & (32),\ (33),\ (34),\ (35) \end{array} \tag{41}$$

The principal aim to solve this problem is to find $\Delta\boldsymbol{\rho}$ and $\Delta\hat{\boldsymbol{c}}$ that minimizes g_X. The values specific to each of the possibilities, $\Delta\boldsymbol{X}^{(p)}$ as well as $\Delta\boldsymbol{\tau}_{\mathsf{A}}^{(p)}$, are determined so as to satisfy the geometrical and equilibrium conditions for the p-th possible kinematic state.

Introducing $\Delta\boldsymbol{q} = [\Delta\boldsymbol{\rho}^T, \Delta\hat{\boldsymbol{c}}^T]^T$, Eqs.(32) and (33) are rewritten as

$$\boldsymbol{A}^{(p)}\Delta\boldsymbol{q} + \boldsymbol{J}^{(p)}\Delta\boldsymbol{v}^{(p)} = \boldsymbol{y}^{(p)} \tag{42}$$

where

$$\boldsymbol{A}^{(p)} = \begin{bmatrix} 0 & \dfrac{\partial \boldsymbol{F}^{(p)}}{\partial \hat{\boldsymbol{c}}} \\ \boldsymbol{B}_{\mathsf{A}^{(p)}} & 0 \end{bmatrix} \tag{43}$$

is the coefficient matrix of $\Delta\boldsymbol{q}$ specific to the p-th possibility, with the boolean matrix $\boldsymbol{B}_{\mathsf{A}^{(p)}}$ to extract the taut wire elements corresponding to $\mathsf{A}^{(p)}$ and

$$\Delta\boldsymbol{y}^{(p)} = \begin{bmatrix} -\boldsymbol{F}_{\epsilon}^{(p)} - \dfrac{\partial \boldsymbol{F}}{\partial \boldsymbol{\tau}_{\mathsf{S}}}^{(p)} \Delta\boldsymbol{\tau}_{\mathsf{S}}^{(p)} \\ \boldsymbol{\rho}_{\mathsf{A}^{(p)}} - \boldsymbol{l}_{\mathsf{A}}^{(p)} \end{bmatrix} \tag{44}$$

is consisting of the right-hand sides of Eqs.(32) and (33), which is also specific to the p-th possibility. Jacobian $\boldsymbol{J}^{(p)}$ and vector $\Delta\boldsymbol{v}^{(p)}$ are respectively corresponding to $\boldsymbol{J}$ and $\Delta\boldsymbol{v}$ in Eqs.(16) and (17) and specific to the p-th possibility as well. The objective function g of problem (41) is also rewritten as

$$g = \frac{1}{2}\Delta\boldsymbol{q}^T\boldsymbol{C}_q\Delta\boldsymbol{q} + \frac{1}{P'}\sum_{p=1}^{P'}\frac{1}{2}\left(\Delta\boldsymbol{v}^{(p)} - \Delta\underline{\boldsymbol{v}}^{(p)}\right)^T\boldsymbol{C}_v^{(p)}\left(\Delta\boldsymbol{v}^{(p)} - \Delta\underline{\boldsymbol{v}}^{(p)}\right) \tag{45}$$

where

$$\boldsymbol{C}_q = \begin{bmatrix} K_\rho\boldsymbol{I} & 0 \\ 0 & K_{\hat{c}}\boldsymbol{I} \end{bmatrix} \tag{46}$$

$$\boldsymbol{C}_v^{(p)} = \begin{bmatrix} K_x\boldsymbol{I} & 0 & 0 \\ 0 & K_\theta\boldsymbol{I} & 0 \\ 0 & 0 & K_\tau\boldsymbol{I}^{(p)} \end{bmatrix} \tag{47}$$

The dimension of identity matrix $\boldsymbol{I}^{(p)}$ in the above equation corresponds to the number of assumed taut wires $\mathrm{Dim}(\mathsf{A}^{(p)})$. On the basis of these representations, the inverse kinematics problem in minimization form (41) is rewritten as follows:

$$\text{Minimize} \quad g \quad \text{with respect to} \quad \Delta\boldsymbol{q}, \Delta\boldsymbol{v}^{(p)}\ (p = 1, \cdots, P') \quad \text{subject to} \quad (34),\ (35),\ (42) \tag{48}$$

It should be noted that the solution of this problem significantly depends on the assumed pattern of tension states $\mathsf{A}^{(p)}$ and $\mathsf{S}^{(p)}$ $(p = 1, \cdots, P')$ of the P' possibilities in consideration. How to choose the pattern of these tension states is quite important for this incremental inverse kinematics approach.

4. Approach to Inverse Kinematics Problem

Problem (48) consists of objective function (45) in quadratic form, linear constraint (42) and inequality constraints (34) and (35). We develop a solution of minimization problem of this type and apply it to problem (48). An approach to deal with the incremental inverse kinematics problem is also proposed on the basis of a procedure to generate patterns of tension states.

4.1 Solution Based on Assumed Pattern of Tension States

Problem (48) without inequality constraints (34) and (35) is expressed as

$$\text{Minimize} \quad g \quad \text{with respect to} \quad \Delta\boldsymbol{q}, \Delta\boldsymbol{v}^{(p)}\ (p = 1, \cdots, P') \quad \text{subject to} \quad (42) \tag{49}$$

This is a quadratic minimization problem characterized by the linear constraint (42), in which the rows have partially common variables; that is, $\Delta\boldsymbol{q}$ is common to all the rows but $\Delta\boldsymbol{v}^{(p)}$ is specific to the p-th row. Assuming a pattern of tension states of $\mathsf{A}^{(p)}$ and $\mathsf{S}^{(p)}$ $(p = 1, \cdots, P')$ after the incremental step, problem (49) can be solved by means of the procedure dealt with in Appendix A. Obtained $\Delta\boldsymbol{q}$ and $\Delta\boldsymbol{v}^{(p)}$ can also be a feasible solution of problem (48), in the case that $\Delta\boldsymbol{\rho}$, $\Delta\boldsymbol{X}^{(p)}$ and $\Delta\boldsymbol{\tau}^{(p)}$ within $\Delta\boldsymbol{q}$ and $\Delta\boldsymbol{v}^{(p)}$ satisfy inequality constraints (34) and (35) as well.

Accordingly, the incremental inverse kinematics problem is solved and the solution $\Delta\boldsymbol{q} = [\Delta\boldsymbol{\rho}^T, \Delta\hat{\boldsymbol{c}}^T]^T$ is obtained. It should be noted that the optimality of the obtained solution in terms of the objective function g significantly depends on the corresponding assumed pattern of tension states.

4.2 Examining Patterns of Tension State

It is not practical to examine all the patterns of tension states $\mathsf{A}^{(p)}$ and $\mathsf{S}^{(p)}$ $(p = 1, \cdots, P')$, since even in a case of $P' = 3$ or $P' = 4$ which typically occurs for a six-wire system, we have to examine $2^{6\times3} = 262,144$ or $2^{6\times4} = 1.7 \times 10^7$ patterns of tension states in principle. It is clear, however, that the inverse kinematics solution should have more taut wires in order to maintain active kinematical DOFs, since the slack wires are practically non-existent from the viewpoint of kinematic motion. In this study, we propose the following procedure that examines patterns of tension states from that consisting of more taut wires, to that consisting of less taut wires.

1. Introduce tension state A^* and S^* to be adopted as the common starting sets for all of the possible kinematic states. The initial values are given as $\mathsf{A}^* = \{1, 2, \cdots, N\}$ and $\mathsf{S}^* = \phi$ in the case of $N \leq 6$, or adequate sets such that $\mathrm{Dim}(\mathsf{A}^*) = 6$ and $\mathrm{Dim}(\mathsf{S}^*) = N - 6$ in the case of $N > 6$.

2. Set $\mathsf{A}^{(p)} = \mathsf{A}^*$ and $\mathsf{S}^{(p)} = \mathsf{S}^*$ $(p = 1, \cdots, P')$.

3. Solve problem (49) based on the current assumed pattern of tension states $\mathsf{A}^{(p)}$ and $\mathsf{S}^{(p)}$ $(p = 1, \cdots, P')$.

4. In the case that the obtained solution satisfies constraints (34) and (35), adopt the obtained $\Delta\boldsymbol{q}$ as the solution of the incremental inverse kinematics problem.

5. If the obtained solution violates *only* the tension constraint (35), the wire n of maximum violation, $n \in \mathsf{A}^{(q)}$, is transferred to $\mathsf{S}^{(q)}$. Continue from step 3 with updated $\mathsf{A}^{(p)}$ and $\mathsf{S}^{(p)}$ $(p = 1, \cdots, P')$.

6. The obtained solution violates the geometrical constraint (34) for some of the possible kinematic states. The series starting from current A^* and S^* is terminated. Generate next common starting tension state A^* and S^*. Repeat from step 2.

7. If there is no other combination of A^* and S^* to be examined at step 6, the inverse kinematics problem is judged to have no solution.

The approach is to examine patterns of tension states based on an assumed tension state A^* and S^* common for all the P' possibilities $\mathsf{A}^{(p)}$ and $\mathsf{S}^{(p)}$ $(p = 1, \cdots, P')$, which is to be modified in one-by-one manner at step 5, according to the situation of tension constraint violation. The number of combinations of A^* and S^* is limited to 2^N. The modification of pattern of tension states at step 5 is unidirectional, that is, only from taut wire set to slack wire set. The procedure certainly stops.

It should be noted that there can be a possible solution for the incremental inverse kinematics problem even in the case that the procedure cannot find any feasible solution, because the procedure does not examine all of the combinations of pattern of tension states $\mathsf{A}^{(p)}$ and $\mathsf{S}^{(p)}$ $(p = 1, \cdots, P')$.

5. Numerical Experiments by Means of Simulated Platform System

In order to demonstrate the feasibility of the developed incremental inverse kinematics approach, we conduct numerical experiments based on a simulated wire-suspended platform system.

5.1 Assumed Condition

Figure 2(a) shows the initial configuration and the wire numbering of the six-wire system adopted in the following numerical experiments. The size and the mass of the platform are 1m and 100kg; the wires are assumed to be massless. The mass center of the platform coincides with its geometrical center in this initial configuration. The dimension of the room where the system is installed is 6(W) × 6(D) × 3(H)m. In the case that the uncertainty is taken into account in the form of an interval of ±0.01m for the wire lengths and the mass center position, the possible kinematic states shown in Figure 2(b) are obtained by means of the incremental forward kinematics calculation with $\Delta\boldsymbol{\rho} = 0$ and $\Delta\hat{\boldsymbol{c}} = 0$; the number of possible kinematic states in this configuration is 25. Slack wires are represented by broken lines.

Figure 2(c) shows the initial configuration of the simulated platform, which is corresponding to the configuration shown in Figure 2(a). This platform system has randomly generated initial error within a range of ±0.01m for the wire lengths and the mass center position. Stiffness of the wire is assumed as $EA = 100$MN; the value is not used in the forward and inverse kinematics calculations but adopted for the calculation of kinematic motion of this simulated practical platform. The calculation is performed based on the steepest descent method which continuously searches the local minima of the sum of the potential energy of gravity and the strain energy of the wires.

Among P possibilities in each incremental step obtained by means of the forward kinematics calculation, P' kinematic states having all the taut wires of the simulated platform are taken into consideration for the inverse kinematics calculation. The condition is expressed as $\mathsf{A}^{(p)} \supset \mathsf{A}^{Simul.}$ for any kinematic state p to be taken into account, where $\mathsf{A}^{Simul.}$ is the taut wire set of the simulated platform. This information is obtained by means of binary-valued wire tension sensors, which are assumed to be installed on the simulated platform in this study. The threshold tension value of the sensor is 150N; the sensing result is obtained in terms of the calculated wire tension of the simulated platform including a measurement noise of ±50N. The threshold of the adopted binary tension sensor is assumed to be of relatively high value. This is because in order to take into account the influence of elasticity of wires of the simulated practical platform, which is not taken into account in the forward and inverse kinematics calculations.

5.2 Simulation Results

Figures 3(a) and (b) show example simulated motions of the platform introduced as in Figure 2(c), based on the proposed inverse kinematics approach. The wire lengths as well as the platform mass center position are adopted as the articulation variables in these motions. The configuration shown in Figure 3(a) is attained based on a translational target motion of 1m right and 1m up from the initial configuration shown in Figure 2(c). The configuration shown in Figure 3(b) is attained based on an additional rotational target motion of 30deg clockwise. Figures 4(a) and (b) show the attained configurations corresponding to the same target motions; however, only the wire lengths are adopted as the articulation variables in this case.

The penalty coefficients K_x and K_θ and the weight coefficients K_ρ, $K_{\hat{c}}$ and K_τ adopted in the inverse kinematics calculations are $K_x = K_\theta = 1.0 \times 10^4$, $K_\rho = 1.0 \times 10^2$, $K_{\hat{c}} = 1.0 \times 10^4$ and $K_\tau = 1.0 \times 10^{-8}$, respectively. The large value of $K_{\hat{c}}$ compared to K_ρ is determined to suppress undesirable large motion of platform mass center position. The particularly small value of K_τ is because we are currently not imposing any limitation on the wire tension values. It should be noted, however, that $K_\tau = 0$ cannot be used even in this case in order to apply the solution procedure dealt with in Appendix A. The number of incremental steps for the forward and inverse kinematics calculations is 200 for both of the translational and rotational motions.

The obtained configurations of the simulated platform shown in Figures 3(a) and (b) are considered to be acceptable in view of the circumstances of the introduced initial error and the corresponding fluctuated initial configuration shown in Figure 2(c). In the case of the motion based only on the adjustment of wire lengths, the degree of attainment of the target motions shown in Figures 4(a) and (b) is lower than the case shown in Figures 3(a) and (b), especially concerning the platform orientation. This is because the right-side wires 1 and 6 cannot push down the right edge of the platform in order to attain the horizontal as well as the right-leaning configurations, since the wires cannot take any compressive force. These results well demonstrate the influence and the importance of the mass distribution of the platform in the case of the mechanical system of this type.

Figures 3(c) and 4(c) show the confined possible configurations to be taken into consideration for the inverse kinematics calculation respectively corresponding to the configurations of the simulated platform shown in Figures 3(b) and 4(b). In both cases, there is a single slack-judged wire as shown in Figures 3(b) and 4(b). The tension value of one of the rest five taut wires of the simulated platform shown in Figure 3(b) is, however, 83N and is judged as slack based on the assumed binary-valued tension sensor; that is, the number of taut wires used for the confinement process is four instead of five. This is the reason that more possibilities are to be taken into consideration for the inverse kinematics in the case of the configuration shown in Figure 3(c).

Figure 5 shows an example of terminated motion due to the failure of the inverse kinematics calculation. The intended motion of the platform is a translation of 3m right and 1m up from the initial configuration shown in Figure 2(c), in 400 incremental steps. The inverse kinematics fails in this case at the 368th step since the procedure cannot find any feasible solution of the minimization problem (48). The reason is as follows. The tension of rear central wire 2 of the simulated platform is only 16N and determined as slack by means of the assumed binary tension sensor. Accordingly, all of existing nine possibilities in the step obtained as the forward kinematics calculation have to be taken into account for the inverse kinematics calculation. It is as a matter of course that the attained configuration is nearly at the rightmost feasible position of the platform, since the wires can only take a tensile force. In other words, the crucial reason of this failure is not due to the inverse kinematics procedure itself, but due to the intrinsic limitation of wires that any of them cannot *push* the platform in order to attain a more rightward

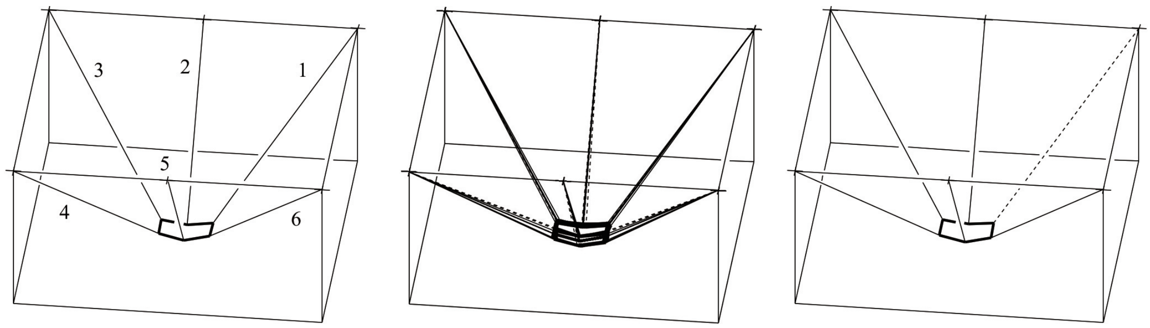

(a) Without uncertainty (wire numbering)
$\boldsymbol{X} = [\ 0.000, 0.000, 0.000$ (m), $0.0, 0.0, 0.0$ (deg) $]$

(b) Uncertainty taken into account
(superimpose of 25 configurations)

(c) Simulated practical platform
$\boldsymbol{X} = [\ -0.000, -0.017, -0.003$ (m), $4.2, -0.7, -1.0$ (deg) $]$

Figure 2. Six-wire system and initial configuration

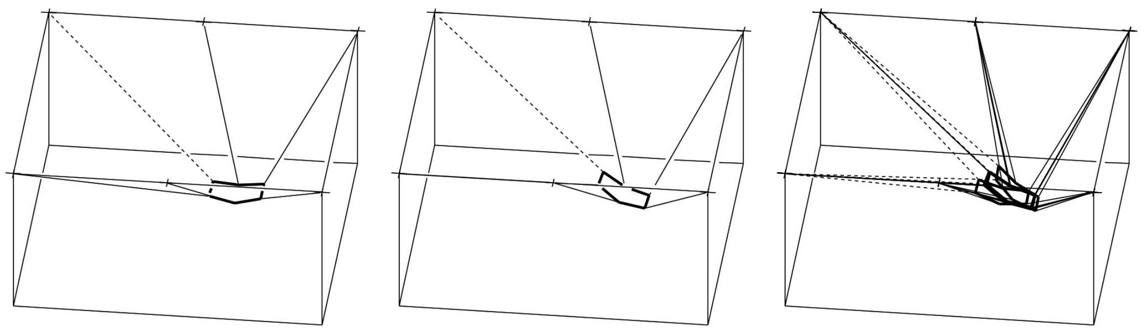

(a) Target: move 1m right, 1m up
$\boldsymbol{X} = [\ 0.997, -0.005, 0.995$ (m), $3.6, -1.1, -1.3$ (deg) $]$

(b) Target: rotate 30deg clockwise
$\boldsymbol{X} = [\ 0.976, 0.015, 0.986$ (m), $-0.5, 24.8, -3.7$ (deg) $]$

(c) Example confined possibilities
(superimpose of 5 configurations)

Figure 3. Kinematic motion using mass center position as well

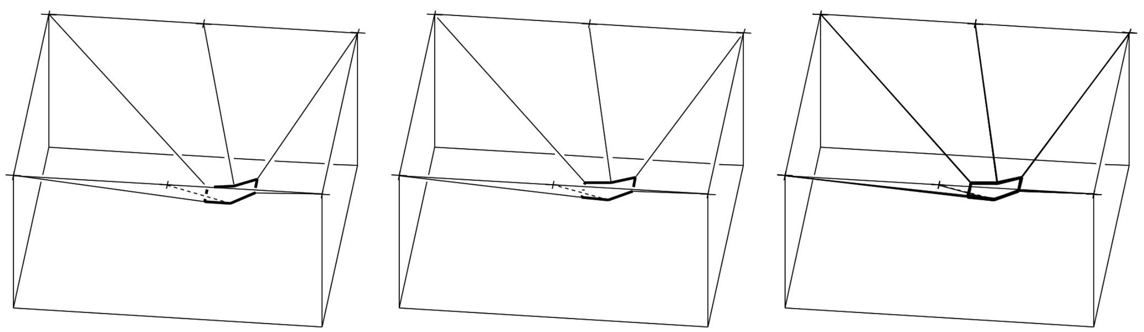

(a) Target: move 1m right, 1m up
$\boldsymbol{X} = [\ 0.913, -0.008, 1.027$ (m), $2.7, -15.4, -0.3$ (deg) $]$

(b) Target: rotate 30deg clockwise
$\boldsymbol{X} = [\ 0.747, -0.012, 1.087$ (m), $3.0, -11.9, -0.3$ (deg) $]$

(c) Example confined possibilities
(superimpose of 2 configurations)

Figure 4. Kinematic motion based only on wire lengths adjustment

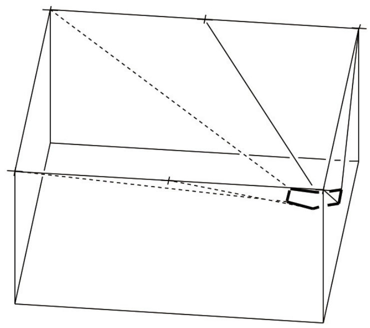

Figure 5. Terminated motion due to failure of inverse kinematics
$\boldsymbol{X} = [\ 2.483, -0.004, 0.908\ (\mathrm{m}), -0.5, -2.6, -0.4\ (\mathrm{deg})\ ]$

position. We use the platform mass center position as the articulation variable as well in this kinematic motion; it is confirmed that the mass center is placed nearly at the right edge of the platform in the configuration shown in Figure 5.

6. Concluding Remarks

We have dealt with an incremental inverse kinematics approach for wire-suspended parallel mechanical systems. The incremental forward kinematics calculation of this type of mechanical system results in plural possibilities, due to the conspicuous mechanical characteristic of wire. In the current study, the formulation of the inverse kinematics problem in an incremental form was developed based on the many-worlds interpretation approach adopted in the previous study. The displacement of the mass center position of the platform is also taken into consideration in addition to the change in wire lengths. The problem has the form of a quadratic minimization problem, which is characterized by the partially common variables. The solution of the problem in general form is given in Appendix A. We also developed the procedure to solve the inverse kinematics problem by examining the possible patterns of tension states.

The developed inverse kinematics approach is quite general. It can be applied to wire-suspended platforms of various numbers of wires, various placements of connection points of wires and various patterns of mass distribution of platform. The feasibility of the proposed incremental inverse kinematics has been demonstrated based on the numerical experiments. The simulated wire-suspended platform is assumed to have error in wire lengths and mass center position and to be equipped with the binary-valued tension sensors. On the basis of this condition, the developed approach was able to generate the intended kinematic motion. The influence as well as the significance of the position of platform mass center was also demonstrated.

Since the developed inverse kinematics problem has a combinatorial nature, we introduce the common initial tension state and confine significantly the patterns of tension states to be examined. This can lead to a condition that the approach cannot find any solution within the examined patterns, but there can exist some solution within the non-examined patterns. Although this is an issue of trade-off, developing an approach that examines more patterns of tension states is considered to be one of the future works.

The wire-suspended platform system has the intrinsic kinematic limitation due to the mechanical condition, as shown in Figure 5. From this point of view, another future works is the design of the platform system in terms of the number of wires, the placement of the connection points and the platform mass distribution taking some specific applications into consideration.

Appendix A. Partially Common Quadratic Minimization

Problem (49) can be expressed in the following general form of partially common quadratic minimization problem:

$$\begin{aligned}
\text{Minimize} \quad & g = \frac{1}{2}(\boldsymbol{x} - \underline{\boldsymbol{x}})^T \boldsymbol{N}_x (\boldsymbol{x} - \underline{\boldsymbol{x}}) + \sum_{i=1}^{n} \frac{1}{2}(\boldsymbol{y}_i - \underline{\boldsymbol{y}}_i)^T \boldsymbol{N}_i (\boldsymbol{y}_i - \underline{\boldsymbol{y}}_i) \\
& \text{with respect to} \quad \boldsymbol{x}, \boldsymbol{y}_i \ (i = 1, \cdots, n) \\
& \text{subject to} \quad \boldsymbol{A}_i \boldsymbol{x} + \boldsymbol{B}_i \boldsymbol{y}_i = z_i \ (i = 1, \cdots, n)
\end{aligned} \tag{50}$$

Introducing Lagrange multipliers $\boldsymbol{\lambda}_1, \cdots, \boldsymbol{\lambda}_n$, this problem is rewritten as

$$\text{Minimize} \quad g' = g + \sum_{i=1}^{n} \boldsymbol{\lambda}_i^T (\boldsymbol{A}_i \boldsymbol{x} + \boldsymbol{B}_i \boldsymbol{y}_i - z_i) \quad \text{with respect to} \quad \boldsymbol{x}, \boldsymbol{y}_i, \boldsymbol{\lambda}_i \ (i = 1, \cdots, n) \tag{51}$$

Differentiating g' with respect to $\boldsymbol{x}$ and $\boldsymbol{y}_i$ and solving for them, we obtain

$$\boldsymbol{x} = \underline{\boldsymbol{x}} - \boldsymbol{N}_x^{-1} \sum_{i=1}^{n} \boldsymbol{A}_i^T \boldsymbol{\lambda}_i \tag{52}$$

$$\boldsymbol{y}_i = \underline{\boldsymbol{y}}_i - \boldsymbol{N}_i^{-1} \boldsymbol{B}_i^T \boldsymbol{\lambda}_i \tag{53}$$

Differentiation of g' with respect to $\boldsymbol{\lambda}_i$ gives

$$\boldsymbol{A}_i \boldsymbol{x} + \boldsymbol{B}_i \boldsymbol{y}_i - z_i = 0 \tag{54}$$

Substituting Eqs.(52) and (53) for Eq.(54), we obtain

$$\boldsymbol{A}_i \left(\underline{\boldsymbol{x}} - \boldsymbol{N}_x^{-1} \sum_{j=1}^{n} \boldsymbol{A}_j^T \boldsymbol{\lambda}_j \right) + \boldsymbol{B}_i (\underline{\boldsymbol{y}}_i - \boldsymbol{N}_i^{-1} \boldsymbol{B}_i^T \boldsymbol{\lambda}_i) - z_i = 0 \tag{55}$$

This equation is modified as

$$\sum_{j=1}^{n} \boldsymbol{A}_i \boldsymbol{N}_x^{-1} \boldsymbol{A}_j^T \boldsymbol{\lambda}_j + \boldsymbol{B}_i \boldsymbol{N}_i^{-1} \boldsymbol{B}_i^T \boldsymbol{\lambda}_i = \boldsymbol{A}_i \underline{\boldsymbol{x}} + \boldsymbol{B}_i \underline{\boldsymbol{y}}_i - z_i \tag{56}$$

Rearranging Eq.(56) for $i = 1, \cdots, n$, we obtain

$$\sum_{j=1}^{n} \boldsymbol{C}_{ij} \boldsymbol{\lambda}_j = \boldsymbol{A}_i \underline{\boldsymbol{x}} + \boldsymbol{B}_i \underline{\boldsymbol{y}}_i - z_i \ (i = 1, \cdots, n) \tag{57}$$

where

$$\boldsymbol{C}_{ij} = \begin{cases} \boldsymbol{A}_i \boldsymbol{N}_x^{-1} \boldsymbol{A}_i^T + \boldsymbol{B}_i \boldsymbol{N}_i^{-1} \boldsymbol{B}_i^T & (i = j) \\ \boldsymbol{A}_i \boldsymbol{N}_x^{-1} \boldsymbol{A}_j^T & (i \neq j) \end{cases} \tag{58}$$

Solving linear equations (57) and substituting obtained $\boldsymbol{\lambda}_1, \cdots, \boldsymbol{\lambda}_n$ for Eqs.(52) and (53), we obtain the solution $\boldsymbol{x}$, $\boldsymbol{y}_1, \cdots, \boldsymbol{y}_n$ of problem (50).

It should be noted that norm matrices $\boldsymbol{N}_x$ and $\boldsymbol{N}_i$ $(i = 1, \cdots, n)$ must not be singular in this solution procedure.

References

Agahi, M., & Notash, L. (2009). Redundancy resolution of wire-actuated parallel manipulators. *Transactions of the Canadian Society for Mechanical Engineering, 33*(4), 561–573.

Albus, J., Bostelman, R., & Dagalakis, N. (1992). The NIST robocrane. *Journal of Research of the National Institute of Standards and Technology, 97*(3), 373–385. http://dx.doi.org/10.6028/jres.097.016

Borgstrom, P. H., Borgstrom, N. P., Stealey, M. J., Jordan, B., Sukhatme, G. S., Batalin, M. A., & Kaiser, W. J. (2009). Design and implementation of NIMS3D, a 3-D cabled robot for actuated sensing applications. *IEEE Transactions on Robotics, 25*(2), 325–339. http://dx.doi.org/10.1109/TRO.2009.2012339

Bosscher, P., Riechel, A. T., & Ebert-Uphoff, I. (2006). Wrench-feasible workspace generation for cable-driven robots. *IEEE Transactions on Robotics, 22*(5), 890–902. http://dx.doi.org/10.1109/TRO.2006.878967

Carricato, M. (2013). Direct geometorico-static problem of underconstrained cable-driven parallel robots with three cables. *Journal of Mechanisms and Robotics, 5*(3), Paper 031008. http://dx.doi.org/10.1115/1.4024293

Carricato, M., & Merlet, J.-P. (2013). Stability analysis of underconstrained cable-driven parallel robots. *IEEE Transactions on Robotics, 29*(1), 288–296. http://dx.doi.org/10.1109/TRO.2012.2217795

Ghasemi, A., Eghtesad, M. & Farid, M. (2009). Workspace analysis for planar and spatial redundant cable robots. *Journal of Mechanisms and Robotics, 1*(4), Paper 044502. http://dx.doi.org/10.1115/1.3211026

Hanahara, K. (2015). Incremental forward kinematics of wire-suspended parallel mechanical system (a many-worlds interpretation approach). *Journal of Mechanisms and Robotics, 7*(4), Paper 041021. http://dx.doi.org/10.1115/1.4030163

Hiller, M., Fang, S., Mielczarek, S., Verhoeven, R., & Franitza, D. (2005). Design, analysis and realization of tendon-based parallel manipulators. *Mechanism and Machine Theory, 40*, 429–445. http://dx.doi.org/10.1016/j.mechmachtheory.2004.08.002

Merlet, J.-P. (2006). *Parallel Robots* (2nd ed.). Springer.

Moore, R. E., Kearfott, R. B. & Cloud, J. J. (2009). *Introduction to Interval Analysis*. SIAM.

Oh, S.-R., & Agrawal, S. K. (2005). Cable suspended planar robots with redundant cables: controllers with positive tensions. *IEEE Transactions on Robotics, 21*(3), 457–465. http://dx.doi.org/10.1109/TRO.2004.838029

Perreault, S., & Gosselin, C. M. (2008). Cable-driven parallel mechanisms: application to a locomotion interface. *Journal of Mechanical Design, 130*, Paper 102301. http://dx.doi.org/10.1115/1.2965607

Pusey, J., Fattah, A., Agrawal, S., & Messina, E. (2004). Design and workspace analysis of a 6-6 cable-suspended parallel robot. *Mechanism and Machine Theory, 39*, 761–778. http://dx.doi.org/10.1016/j.mechmachtheory.2004.02.010

Roberts, R. G., Graham, T., & Lippitt, T. (1998). On the inverse kinematics, statics, and fault tolerance of cable-suspended robots. *Journal of Robotic Systems, 15*(10), 581–597. http://dx.doi.org/10.1002/(SICI)1097-4563(199810)15:10<581::AID-ROB4>3.0.CO;2-P

Stewart, D. (1965-66). A platform with six degrees of freedom. *Proceedings of Institution of Mechanical Engineers, 180*(15), Part 1, 371–386.

Tadokoro, S., Verhoeven, R., Zwiers, U., Hiller, M. & Takemura, F. (2003). Kinematic identification method for cable-driven rescue robots in unstructured environments. *Journal of Robotics and Mechatronics, 15*(5), 571–578.

Vaidman, L. (2008). Many-worlds interpretation of quantum mechanics. *The Stanford Encyclopedia of Philosophy* (Fall 2008 ed.). Retrieved from http://plato.stanford.edu/archives/fall2008/entries/qm-manyworlds/ .

Yamaguchi, D., Tagawa, Y., Hayatsu, M., & Yamada, M. (2004). Sequential identification technique of jacobian matrix for a power-assisted lifter using wire-driven parallel mechanism. *Journal of Robotics and Mechatronics, 16*(3), 228–236.

Copyrights